Title	Switching of Cu/MoOx/TiN CBRAM occurred at MoOx/TiN interface
Author(s)	Arita, Masashi; Ohno, Yuuki; Takahashi, Yasuo
Citation	Physica Status Solidi A applications and materials science, 213(2), 306-310 https://doi.org/10.1002/pssa.201532414
Issue Date	2016-02
Doc URL	http://hdl.handle.net/2115/64496
Rights	This is the peer reviewed version of the following article: Physica Status Solidi (A) : applications and materials science, Volume 213, Issue 2, Pages 306–310, February 2016, which has been published in final form at http://doi.org/10.1002/pssa.201532414. This article may be used for non-commercial purposes in accordance with Wiley Terms and Conditions for Self-Archiving.
Type	article (author version)
File Information	Arita_pssa_Final_Correction for HUSCAP..pdf

Switching of Cu/MoO$_x$/TiN CBRAM occurred at MoO$_x$-TiN interface

Masashi Arita [*,1], **Yuuki Ohno** [1], **and Yasuo Takahashi** [1]

[1] Graduate School of Information Science and Technology, Hokkaido University, Kita-14, Nishi-9, Kita-ku, 060-0814 Sapporo, Japan.

Received ZZZ, revised ZZZ, accepted ZZZ

Keywords ReRAM, CBRAM, conductive filament, in-situ transmission electron microscopy

---

* Corresponding author: arita@nano.ist.hokudai.ac.jp, Phone/Fax: +81 11 706 6457

For dynamical observation of CBRAM microstructure, *in-situ* transmission electron microscopy (*in-situ* TEM) was performed on Cu/MoO$_x$/TiN during the resistive switching. It was confirmed that local area near the MoO$_x$/TiN interface contributes to resistive switching. The Cu deposit at the bottom of the MoO$_x$ layer swelled into the oxidized thin layer of the TiN bottom electrode, and thin filament with 3-5 nm in diameter was formed in the *Set* process. The reversal change was seen in the *Reset* process. Increasing the switching power, microstructure change in the MoO$_x$ layer was also seen, and the CBRAM film was finally destructed.

1 Introduction The resistive random access memory (ReRAM) has been intensively investigated to develop next-generation nonvolatile memories as well as artificial neurons [1–4]. Solid electrolyte sandwiched between an active (e.g. Cu or Ag) top electrode (TE) and an inactive (e.g. Pt and TiN) bottom electrode (BE) is one of the candidates used for ReRAMs, which are called as the conductive bridging RAM (CBRAM), the programmable metallization cell (PMC), the atom switch or the solid electrolyte ReRAM [5-10]. The switching mode of this system is bipolar requiring both voltage polarities. Its resistance changes from the high resistance state (HRS) to the low resistance states (LRS) by applying positive voltage to the TE (*Set* procedure). The redox reaction is thought to generate a Cu conductive filament (CF) in the solid electrolyte switching layer, and LRS is achieved when this filament connects the TE and the BE. On the other hand, with negative voltage, the CF ruptures and HRS is recovered (*Reset* procedure). While this operation model based on the electrochemical discussion is quite plausible, details of CBRAM switching is still ambiguous, such as microstructure evolution during the operation.

Considering practical usage of ReRAM devices in electric circuits, elucidation of the switching mechanism is inevitable to guarantee the reliability of the ReRAM operation. To overcome this problem, *in-situ* transmission electron microscopy (TEM) has been applied on CBRAMs [11–17] as well as other ReRAM families [18-21], and CF formation during the *Set* operation was experimentally confirmed. Recently, Kudo *et al.* [16] succeeded to achieve multiple current-voltage (*I-V*) switching cycles of Cu/MoO$_x$/TiN CBRAM in TEM, and CF erasure was observed during the *Reset* operation in addition to CF appearance at *Set*. However, no remarkable change in microstructure was seen at the switching moment of the *I-V* curve. Additional voltage application was required after *Set* and *Reset* to clearly observe the CF growth and erasure, respectively. These will be called as *over-Set* and *over-Reset* in this report, respectively. Therefore, it can be expected that the ReRAM switching occurs locally in the CF. Considering the interfaces between the Cu CF and two electrodes, Cu(CF)-Cu(TE) is more or less a homogeneous junction, because both side of the junction are Cu. On the other hand, the junction of Cu(CF)-TiN(BE) is heterogeneous. Thus, observation of the local area around the CF and the BE must be important to investigate the switching operation.

In this work, a Cu/MoO$_x$/TiN CBRAM was investigated by *in-situ* TEM paying attention not to perform strong *over-Set* and *over-Reset*. The microstructure change near the lower end of the MoO$_x$ layer was preferentially observed. A thin CF having a diameter of 3-5 nm appeared and disappeared in the oxidized layer of the TiN(BE). Resistive switching in a local region was experimentally confirmed.

2 Experimental procedure The Pt/Cu(TE)/MoO_x film was RF-sputter deposited at room temperature (RT) on TiN(BE)/Si whose surface had been treated by oxygen plasma for cleaning. The solid electrolyte MoO_x layer (50-nm-thick) was prepared by reactive RF sputtering (Ar-20% O_2). It was cut in small pieces (2.5 mm (length) × 100 μm (width) × 525 μm (thickness)), and TEM samples were fabricated by the ion shadow method for about one hour, which is an Ar ion milling method (5 kV, 1 mA, beam diameter ~ 2 mm) using carbon particles as the mask material [22]. A TEM image of the sample investigated in this work is presented in Fig. 1, which shows a clear layer stacking. The CBRAM sample had a cone shape with some irregularity. Dark contrast around A came from thicker region caused by this irregularity. The slightly bright linear contrast between MoO_x and TiN/Ti corresponds to oxidized TiN (abbreviated as ox-TiN in this report) by oxygen plasma pre-treatment described above, which was confirmed by the XPS measurement. This is analogous structure of the double layer CBRAM which shows sharp *I-V* switching curves [6, 7].

In-situ TEM was performed by using a JEM-2010 microscope (200 kV, 10^{-5} Pa, C_s = 0.5 mm) attached with a home-made piezo holder [19, 21]. The CBRAM sample was fixed in this holder, and a movable Pt-Ir probe was contacted to the Pt/Cu (TE) as shown in Fig. 1. The *I-V* measurements were done with voltage to the TE by using a Yokogawa GS820 source-measure-unit (SMU), where the voltage sweep rate was typically 0.79 V/s. Image dynamics was recorded with a CCD camera (30 frames s^{-1}). The image contrast was enhanced non-linearly to clearly identify faint contrast of the fine CF. Contrast change during switching cycles was seen mainly in region B of Fig. 1. Processed videos are presented as supporting information; S1.3gp, S2.3gp, S3.3gp and S4.3gp.

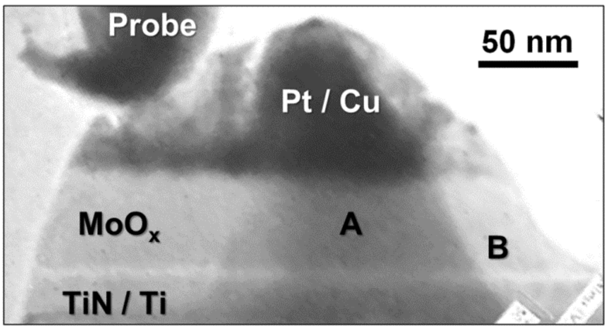

Figure 1 Cross-sectional TEM image of the investigated sample, which was extracted from the video. Dark contrast around A is thought to be caused by the irregularity of the sample shape. Clear stacking is seen. Contrast change in ReRAM switching cycles was seen in region B.

3 Results and discussion The *I-V* switching curves from the pristine state (the first to the fourth cycle) are shown in Fig. 2, which were measured in TEM with a compliance current of I_{comp} = 50 μA. The curve was reproducible in these switching cycles. While the switching was not so abrupt, *Set* switching started at V_{Set} = 1.2 - 1.3 V, and *Reset* switching occurred at V_{Reset} = -1.2 to -1.8 V. The first *Set* cycle is usually the initialization process to form a template of CF and is called as *Forming*. While the voltage to achieve *Forming* (V_{Form}) is usually higher than V_{Set} in subsequent switching cycles, it was nearly the same as V_{set} in Fig. 2. The reason of this reduction in V_{Form} (or forming-free switching) can be inferred from the *in-situ* TEM result

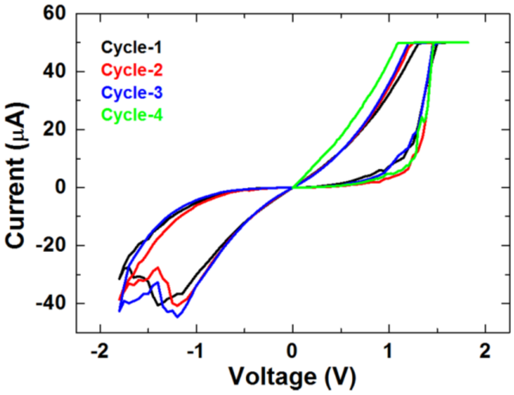

Figure 2 *S*witching curves of the first to the fourth cycles.

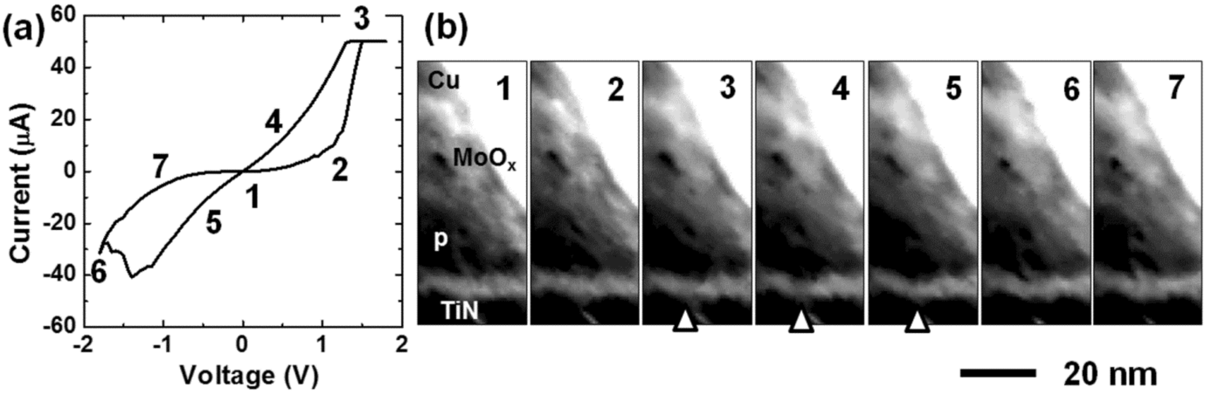

Figure 3 First *Set/Reset* switching cycle. (a) *I-V* switching curve, and (b) corresponding TEM images extracted from a video. At the lower part of "p" (arrow), faint contrast change is seen in states 3 and 4 (*Set*) and in states 6 and 7 (*Reset*). This contrast change can be identified more easily in the video presented as supporting information (S1.3gp).

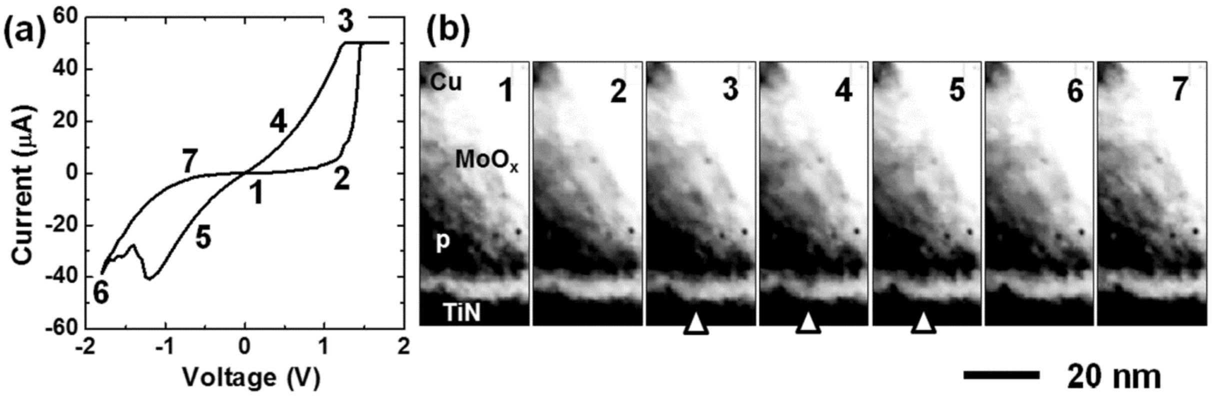

Figure 4 Second *Set/Reset* switching cycle. (a) *I-V* switching curve, and (b) corresponding TEM images extracted from a video. Faint contrast of a filament is seen at the arrowed position in states 3-5 as occurred in the first cycle (Fig. 3). A video file is attached as supporting information (S2.3gp).

of the first cycle (Fig. 3). In state 1 of Fig. 3(a), the CBRAM was in the HRS. However, there was already a region with dark contrast (marked by "p" in Fig. 3(b)-1) just above the TiN BE, which may correspond to a Cu deposit as analysed in our previous works [11, 16]. Thermadam *et al.* investigated heat treatment of Cu/SiO_2/BE (TiN or W) [23]. They reported Cu diffusion into SiO_2 and its segregation at the SiO_2/BE interface, and reduction of V_{Form} was discussed. Though no special heat treatment was performed in the present work, the ion shadow process (a kind of Ar ion milling) to prepare the TEM sample may cause temperature increase, a similar thing to Ref. 23 is expected to occur. This is a possible reason of Cu deposit in MoO_x near the bottom interface with TiN. The increase in temperature may differ for every sample, because sample positioning relative to the Ar beam was not so accurate. Thus the amount of Cu deposit may differ for every sample.

While there was no change in the TEM image until state 2 of Fig. 3(b), the bottom edge of the Cu deposit marked with "p" swelled out downwards into ox-TiN (~5-nm-thick) in state 3 after the *Set* switching (arrowed position in Fig. 3(b)-3). At the same time, a faint contrast indicating a filament appeared to bridge the deposit and TiN. The swelling of the deposit and the filament were kept in states 4 and 5 (arrows). After *Reset* switching around V_{Reset} ~ -1.5 V, this faint contrast disappeared, and the swelled part shrunk upwards (states 6 and 7). This sequence can be seen dynamically in a video S1.3gp. To confirm this local switching position, the video of the second cycle was analysed in the same way. The result is shown in Fig. 4, whose contrast was coordinated with different parameters from those of Fig. 3, and a video S2.3gp. At almost the same place as that in Fig. 3, swelling occurred and the filament appeared. The filament width estimated from Figs. 3(b) and 4(b) was roughly 3-5 nm while its visual size depends on degree of contrast enhancement. Such a small filament contributes to ReRAM switching when *over-Set* and *over-Reset* does not happen. Even without a thick CF contacting to the Cu TE, the ReRAM switching was achieved. As mentioned above, Cu is thought to be dissolved in regions of MoO_x other than the CF. Assuming the dissolved Cu are cations, they should move along the electric field generating ionic current and contribute to the current flow through the CBRAM. To check this clearly, the sweep rate was lowered to be 0.32 V/s (half of those in cycles 1-3) in the fourth *Set* cycle. In a video S3.3gp as supporting information, growth of the deposit is clearly seen. In addition, the lower edge of the Cu TE slightly contracted. Cu was surely transferred from the TE to the lower part of the MoO_x layer.

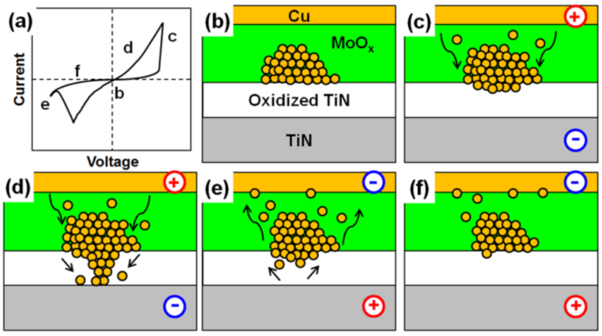

Figure 5 Schematics of (a) an *I-V* switching curve and (b)-(f) corresponding filament formation and rupture. Circles are Cu atoms and ions, and arrows denote the ion movement. Plus and minus signs indicate the polarities of applied voltage.

The schematic *I-V* curve and corresponding microstructure expected from experimental results are shown in Fig. 5. As described above, the surface of the BE was oxidized. The XPS measurement gave a spectrum quite similar to TiO_2. Therefore, this can be classified as a CBRAM with a thin oxide layer as in [6, 7]. There was a deposit in the initial state. There was no clear contrast to confirm this deposit connected to the Cu TE (Fig. 5(b)). *Set* switching occurs when the voltage reaches to "c" in Fig. 5(a), and the lower part of the deposit swells into the oxidized TiN (ox-TiN) layer (Fig. 5(c)). And a filament appears in ox-TiN to connect the deposit and the BE (Fig. 5(d)). Even in this stage, no clear contrast was identified between the deposit and the Cu TE. The current is thought to be contributed by Cu ions drifting along the electric field as described above. Oxygen vacancies as well as electrons may also be listed to contribute the current, though details are obscure. At *Reset*, the fine filament in ox-TiN disappears (Fig. 5(e)), and the swelling part shrinks (Fig. 5(f)). Without *over-Set* and *over-Reset*, thick filament are not formed in MoO_x, and switching seems to occur in thin oxide layer on the BE. Similar thing is expected in the CBRAM having a Pt BE with a thin Ti gluing layer. It was reported that Ti underneath the Pt layer moved to the Pt surface by heat treatment [24]. When Ti on Pt is oxidized there, its structure is quite similar to that of the present sample. The CF in the ox-TiN appeared from Cu to TiN and disappeared from TiN to Cu. This growth/erase direction was reported also in other oxide switching layers such as SiO_2 and ZrO_2, and it is inconsistent to the conventional electrochemical model [1]. To explain this inconsistency, reduction/oxidation of the Cu ions within the oxide layer [13, 14, 25] or the doping/de-doping effect [26] were proposed. Though the details are ambiguous, a similar thing is thought to occur in the ox-TiN layer. It was pointed out that TiO_2 can act as the switching layer of CBRAM and also VCM (valence change memory) by adequate selection of the electrode materials [26]. Thus, a complex switching mechanism contributed by both copper ions and oxygen vacancies may be another possibility to be considered. Further investigation is required to solve this polemic discussion.

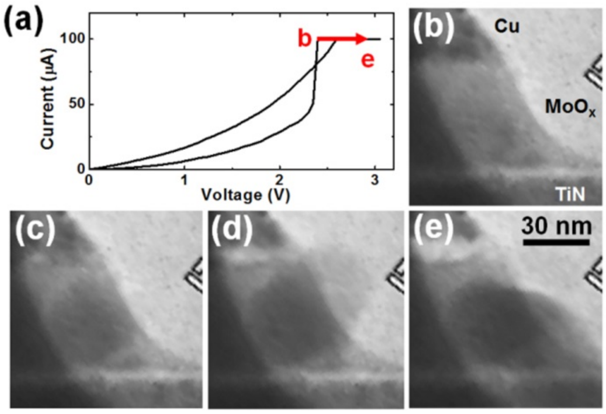

Figure 6 Device destruction with high power injection. (a) The *I-V* curve and (b)-(e) corresponding TEM images extracted from a video (S4.3gp, supporting information) showing the progress of device destruction. From these images, it is confirmed that Cu ions were transported in the MoO_x layer instead of on the surface.

At the end of this section, a process of device destruction is shown to confirm that Cu moved inside the MoO_x layer but not on the surface. After the fourth *Set* process, clear *Set/Reset* switching was not achieved while weak breathing of the deposit was identified during the *I-V* cycles. Lack of switching is thought to be caused by development of the Cu deposit which moved much into the ox-TiN layer as seen in the video (S3.3gp). The *I-V* cycles were repeated with increasing I_{comp} and widening the voltage range. Finally, the sample was destructed as shown in Fig. 6 and in a video (S4.3gp) of the eleventh *I-V* cycle. At the voltage of about 2.4 V, the current sharply reached to "b" (Fig. 6(a)). At this moment, the TEM image did not show any change (Fig. 6(b)). Continuing the voltage application from "b" to "e", a precipitation clearly appeared and gushed out of MoO_x (Figs. 6(c)-(e)). At the same time, the Cu TE got lean. Cu dissolved from TE into MoO_x is thought to break the surface. Because of lack of Cu supplied from the TE, there was a crossover in the *I-V* curve as discussed in a previous report on Cu-GeS [27]. These phenomena seen in the eleventh *Set* cycle can be a proof that the CF and the deposit seen in Figs. 3 and 4 are composed of Cu.

4 Summary and conclusion A CBRAM film composed of $Cu/MoO_x/TiN$ was studied by *in-situ* TEM to investigate the microstructure evolution during resistive switching. Under the switching condition without generating *over-Set* or *over-Reset*, the local area near the MoO_x/TiN interface contributed to resistive switching. The Cu deposit at the bottom of the MoO_x layer swelled into the ox-TiN layer at the interface, and thin filament with 3-5 nm in diameter was formed there in the *Set* process, while reversal change was seen in the *Reset* process. Increasing the switching power (voltage, current and sweep rate), the microstructure in the MoO_x layer changed. This will lead to the thick CF in solid electrolyte (MoO_x in this case) in addition to the thin CF in ox-TiN as described in previous reports [15, 16].

Acknowledgements This work was supported by KAKENHI by Japan Society of the Promotion of Science (JSPS) (Nos. 25420279, 26630141) and the Mitsubishi Foundation, and partly performed under the Nanotechnology Platform Program.

References

[1] R. Waser, and M. Aono, Nature Mater. **6**, 833 (2007).
[2] H. Akinaga, and H. Shima, Proc. IEEE **98**, 2237 (2010).
[3] A. Chen, *Ionic Memory Technology*, in *Solid State Electrochemistry II: Electrodes, Interfaces and Ceramic Membranes*, 1st ed., edited by V. V. Kharton (Wiley-VCH, Weinheim, 2011).
[4] M. Prezioso, F. Merrikh-Bayat, B. D. Hoskins, G. C. Adam, K. K. Likharev, and D. B. Strukov, Nature **521**, 61 (2015).
[5] M. N. Kozicki, M. Park and M. Mitkova, IEEE Trans. Nanotechnol. **4**, 331 (2005).
[6] D. Lee, D.-j. Seong, H. j. Choi, I. Jo, R. Dong ,W. Xiang, ,S. Oh, M. Pyun, S.-o. Seo, S. Heo, M. Jo, D.-K. Hwang, H. K Park, M. Chang, M. Hasan, and H. Hwang, Tech. Dig. Int. Electron Devices Meet. **2015**, 797–800.
[7] K. Aratani, K. Ohba, T. Mizuguchi, S. Yasuda, T. Shiimoto, T. Tsushima, T. Sone, K. Endo, A. Kouchiyama, S. Sasaki, A. Maesaka, N. Yamada, and H. Narisawa, Tech. Dig. Int. Electron Devices Meet. **2007**, 783–786.

[8] N. Banno, T. Sakamoto, N. Iguchi, H. Sunamura, K. Terabe, }T. Hasegawa, and M. Aono, IEEE Trans. Electron Devices **55**, 3283 (2008).

[9] C. Kügeler, R. Rosezin, R. Weng, R. Waser, S. Menzel, B. Klopstra, and U. Böttger, in *Proceedings of the 9th Conference on Nanotechnology: (IEEE NANO 2009)*, Genoa, Italy, 2009 (IEEE, Piscataway, 2009) pp. 1102–1105.

[10] Y. Bernard, V. T. Renard, P. Gonon, and V. Jousseaume, Microelect. Eng. **88**, 814 (2011).

[11] T. Fujii, M. Arita, Y. Takahashi, and I. Fujiwara, Appl. Phys. Lett. **98**, 212104 (2011).

[12] S.-J. Choi, G.-S. Park, K.-H. Kim, S. Cho, W.-Y. Yang, X.-S. Li, J.-H. Moon, K.-J. Lee, and K. Kim, Adv. Mater. **23**, 3272 (2011).

[13] Q. Liu, J. Sun, H. Lv, S. Long, K. Yin, N. Wan, Y. Li, L. Sun, and M. Liu, Adv. Mater. **24**, 1844 (2012).

[14] Y. Yang, P. Gao, S. Gaba, T. Chang, X. Pan, and W. Lu, Nat. Commun. **3**, 732 (2012).

[15] Y. Ohno, T. Hiroi, M. Kudo, K. Hamada, M. Arita, and Y. Takahashi, IECIE Tech. Rept. **113**, 89 (2014), in Japanese.

[16] M. Kudo, M. Arita, Y. Ohno, and Y. Takahashi, Appl. Phys. Lett. **105**, 173504 (2014).

[17] M. Kudo, M. Arita, Y. Takahashi, K. Ohba, M. Shimuta, and I. Fujiwara, in *Proceedings of IEEE 7th International Memory Workshop*, Monterey, CA, USA, 2015 (IEEE, Piscataway, 2009) pp. 85–88.

[18] Ch. Jooss, J. Hoffmann, J. Fladerer, M. Ehrhardt, T. Beetz, L. Wu, and Y. Zhu, Phys. Rev. B **77**, 132409 (2008).

[19] T. Fujii, H. Kaji, H. Kondo, K. Hamada, M. Arita, and Y. Takahashi, IOP Conf. Ser.: Mater. Sci. Eng. **8**, 012033 (2010).

[20] D.-H. Kwon, K. M. Kim, J. H. Jang, J. M. Jeon, M. H. Lee, G. H. Kim, X.-S. Li, G.-S. Park, B. Lee, S. Han, M. Kim, and C. S. Hwang, Nat. Nanotechnol. **5**, 148 (2010).

[21] T. Fujii, M. Arita, K. Hamada, H. Kondo, H. Kaji, Y. Takahashi, M.Moniwa, I. Fujiwara, T. Yamaguchi, M. Aoki, Y. Maeno, T. Kobayashi, and M. Yoshimaru, J. Appl. Phys. **109**, 053702 (2011).

[22] M. Kudo, M. Arita, Y. Ohno, T. Fujii, K. Hamada, and Y. Takahashi, Thin Solid Films **533**, 48 (2013).

[23] S. P. Thermadam, S. K. Bhagat, T. L. Alford, Y. Sakaguchi, M. N. Kozicki, and M. Mitkova, Thin Solid Films **518**, 3293 (2010).

[24] K. Kinoshita, A. Okano, K. Tsunoda, M. Aoki, and Y. Sugiyama, Appl. Phys. Express **1**, 125001 (2008).

[25] X. Tian, S. Yang, M. Zeng, L. Wang, J. Wei, Z. Xu, W. Wang, and X. Bai, Adv. Mater. **26**, 3649 (2014).

[26] I. Valov, and R. Waser, Adv. Mater. **25**, 162 (2013).

[27] T. Fujii, M. Arita, Y. Takahashi, and I. Fujiwara, J. Mater. Res. **27**, 886 (2012).